Study of the photochemical transformation of 2-ethylhexyl 4-(dimethylamino)benzoate (OD-PABA) under conditions relevant to surface waters

Study of the photochemical transformation of 2-ethylhexyl 4-(dimethylamino)benzoate (OD-PABA) under conditions relevant to surface waters

P. Calza[1], D. Vione[1,2] *, F. Galli[1], D. Fabbri[1], F. Dal Bello[3], C. Medana[3]

[1]*Department of Chemistry, University of Torino, via P. Giuria 5, 10125 Torino, Italy*

[2]*NatRisk Inter-Department Centre, University of Torino, via L. da Vinci 44, 10095 Grugliasco (TO), Italy.*

[3]*Department of Molecular Biotechnology and Health Sciences, University of Torino, via P. Giuria 5, 10125 Torino, Italy*

* Corresponding author: e-mail: davide.vione@unito.it

Abstract

We studied the aquatic environmental fate of 2-ethylhexyl 4-(dimethylamino)benzoate (OD-PABA), a widespread sunscreen, to assess its environmental persistence and photoinduced transformation. Direct photolysis is shown to play a key role in phototransformation, and this fast process is expected to be the main attenuation route of OD-PABA in sunlit surface waters.

The generation of transformation products (TPs) was followed *via* HPLC/HRMS. Five (or four) TPs were detected in the samples exposed to UVB (or UVA) radiation, respectively. The main detected TPs of OD-PABA, at least as far as HPLC-HRMS peak areas are concerned, would involve a dealkylation or hydroxylation/oxidation process in both direct photolysis and indirect

phototransformation. The latter was simulated by using TiO_2-based heterogeneous photocatalysis, involving the formation of nine additional TPs. Most of them resulted from the further degradation of the primary TPs that can also be formed by direct photolysis. Therefore, these secondary TPs might also occur as later transformation intemediates in natural aquatic systems.

Keywords: OD-PABA; sunscreen; photolysis; titanium dioxide; transformation products.

1. Introduction

Sunscreens are widely used compounds that play a preventive action against the damage caused by exposure to ultraviolet light. They are often added to personal care products such as shampoos, body creams, sprays and hair dyes. Furthermore, they also found several industrial applications to prevent photodegradation of polymers and pigments. Due to their widespread use, the occurrence of sunscreens in the environment has been reported in many studies that took into account water, solid and biota samples (Poiger et al., 2004; Rodil and Moeder, 2008; Magi et al., 2013; Kupper et al., 2006; Balmer et al., 2005; Bachelot et al., 2012; Kameda et al., 2011; Goksoyr et al., 2009). In the present study, we focused on 2-ethylhexyl 4-(dimethylamino)benzoate (OD-PABA), also known as Padimate O or Escalol 507, produced upon condensation of 2-ethylhexanol and para-amino benzoic acid (PABA). PABA itself was among the first compounds to be used as sunscreens, but in 2008 it was removed from the list of permitted organic sunscreens in the European Union because of the increasing evidence of its involvement in photo-allergic reactions and estrogenic effects (Schlumpf et al., 2001; Gomez et al., 2005). For the same reason also the PABA derivatives, including OD-PABA, are gradually being replaced by other organic UV filters. A recent study identified OD-PABA metabolites in human urine following its application on skin (Leon-Gonzalez et al., 2011).

OD-PABA can reach surface waters through incomplete degradation in wastewater treatment plants, or directly upon skin contact with water as a consequence of the use of sunscreen lotions during recreational activities. This compound has been found in wastewater and tap water at levels of 2-100 ng/L (Magi et al., 2013; Diaz-Cruz et al., 2012). In environmental waters, in addition to biotransformation, photodegradation by direct and indirect photochemistry is a potentially important attenuation pathway for many xenobiotics. Direct photolysis implies the transformation of a compound upon absorption of sunlight, which triggers *e.g.* bond breaking, photoionisation or excited-state reactivity. In the case of indirect photochemistry, sunlight is absorbed by photoactive compounds (photosensitisers, such as nitrate, nitrite and chromophoric dissolved organic matter, CDOM) that produce reactive transient species such as the hydroxyl radical (•OH), singlet oxygen ($^1O_2$) and CDOM triplet states (^{3}CDOM*) (Canonica et al., 2005; Canonica et al., 2006; Fenner et al., 2013; Mostafa et al., 2013; Mostafa et al., 2014). These reactive transients can be involved in the degradation of xenobiotics, but •OH is also scavenged by natural water components such as DOM, carbonate and bicarbonate (Vione et al., 2014). In contrast, unless the water DOC is very high (Wenk et al., 2013), the main $^1O_2$ sink is the thermal deactivation upon collision with the solvent, while ^{3}CDOM* mainly react with O_2 in aerated surface waters to produce $^1O_2$ (Vione et al., 2014).

The present work aims at assessing the main direct and/or indirect pathways involved in the photochemical attenuation of OD-PABA in sunlit surface waters. This goal was fulfilled by a combination of laboratory studies and photochemical modelling. Such an approach has already proven its suitability to assess the photodegradation kinetics of compounds, for which field data of photochemical attenuation are available for comparison (Vione et al. 2011; De Laurentiis et al., 2012; Marchetti et al., 2013; Fabbri et al., 2015). Furthermore, the main intermediates arising from the prevailing processes of OD-PABA photodegradation were identified. The environmental degradation upon indirect photochemistry was simulated by the use of heterogeneous photocatalysis

with titanium dioxide (TiO_2). This approach has already permitted the identification in natural aquatic samples of several transformation products formed through indirect photolysis processes, as documented in several studies (Calza et al., 2010; Calza et al., 2011; Calza et al., 2013). We preferred TiO_2-based photocatalysis over alternative approaches (*e.g.* the use of triplet sensitisers) to avoid possible interferences potentially arising from the sensitiser transformation products, and to minimise the direct photolysis process under irradiation (*vide infra*).

2. Experimental section

2.1. Materials and reagents

OD-PABA (CAS 21245-02-3, purity grade 98%), methanol (≥99,9%), acetonitrile (≥99,9%), formic acid (99%), NaCl (≥ 99.5%), acetaminophen (APAP, ≥ 99.0%) and anthraquinone-2-sulphonic acid, sodium salt (AQ2S, 97%) were purchased from Sigma Aldrich (Milan, Italy). Rose Bengal was purchased from Alfa Aesar (Karlsruhe, Germany).

Experiments on heterogeneous photocatalysis were carried out using TiO_2-P25. The TiO_2 powder was irradiated and washed with distilled water until no signal due to chloride, sulphate or sodium ions could be detected by ion chromatography, in order to avoid possible interference from ions adsorbed on the photocatalyst.

2.2. Irradiation procedures

2.2.1. Direct photolysis

Due to the low OD-PABA solubility in water, the aqueous solutions were prepared by methanol spiking (Rodil et al., 2009). The aqueous solutions of the sunscreen were prepared by adding, to 100 mL water, a 0.4 mL aliquot of a concentrated methanol solution of OD-PABA (1000 mg/L), in order to have a final concentration of 4 mg/L ($1.4 \cdot 10^{-5}$ M).

Five millilitres of the thus obtained aqueous solutions were introduced into cells of Pyrex glass for the irradiation experiments. UVA irradiation was carried out under a Philips TLK 05 40W lamp, with maximum emission at 365 nm. UVB irradiation made use of a Philips TL 20W/01 RS lamp, with emission maximum at 313 nm. Lamp radiation reached the irradiated solutions mainly from the top. After the scheduled irradiation time, the content of the cells was recovered with 5 mL methanol to desorb the analytes from the cell walls (Li et al., 2007). The use of methanol allowed a nearly quantitative recovery. Alternative tests were carried out with acetonitrile spiking, obtaining fully comparable results as for methanol.

The time evolution data of OD-PABA were fitted with the pseudo-first order kinetic equation $C_t = C_o\, e^{-kt}$, where C_t is the substrate concentration at time t, C_o the initial concentration and k the pseudo-first order degradation rate constant (units of s^{-1}). The initial transformation rate (units of M s^{-1}) is $R_{OD-PABA} = k\, C_o$. The reported error on the rates ($\pm\sigma$) mainly depended on the uncertainty on k, which represents the average of replicate runs. The direct photolysis quantum yield (unitless) was calculated as $\Phi_{OD-PABA} = R_{OD-PABA}(P_a^{OD-PABA})^{-1} \cdot \quad P_a^{OD-PABA} = \int_\lambda p°(\lambda)[1-10^{-\varepsilon_{OD-PABA}(\lambda) b [OD-PABA]}]d\lambda$ (units of Einstein L^{-1} s^{-1}) is the photon flux absorbed by OD-PABA (Braslavsky, 2007), where $p°(\lambda)$ [Einstein L^{-1} s^{-1} nm^{-1}] is the incident spectral photon flux density of lamp radiation into the solution. For these measurements it was used the lamp Philips TL 20W/01 RS (see Figure 1). Morever, $\varepsilon_{OD-PABA}(\lambda)$ [M^{-1} cm^{-1}] is the molar absorption coefficient of the substrate (Figure 1), b = 0.4 cm is the optical path length of radiation in solution, and [OD-PABA] = $1.4 \cdot 10^{-5}$ M is the initial concentration of the substrate.

2.2.2. Indirect photochemistry

The above-described technique of methanol spiking was used in the case of indirect photolysis as well. To determine the second-order reaction rate constants of OD-PABA with •OH, $^1O_2$ and CDOM triplet states, acetaminophen (APAP) was used as model compound because its reaction rate constants with the above transients are known (De Laurentiis et al., 2014). In this case, solutions containing OD-PABA and APAP at equal initial concentration (10 µM for both) were irradiated under suitable conditions (*vide infra*) to produce the transient species X (•OH, $^1O_2$ or ^{3}CDOM*). The time evolution of the OD-PABA and APAP was monitored, and the concentration *vs*. time data were fitted with $C_t = C_o\, e^{-kt}$, calculating the initial rates as already described.

If the degradation of the two substrates is mainly or exclusively accounted for by reaction with X, the ratio of their initial transformation rates can be expressed as follows:

$$\frac{R_{OD-PABA}}{R_{APAP}} = \frac{k_{OD-PABA,X}\,[X][OD-PABA]}{k_{APAP,X}\,[X][APAP]} = \frac{k_{OD-PABA,X}}{k_{APAP,X}} \qquad (1)$$

where $k_{OD-PABA,X}$ and $k_{APAP,X}$ are the second-order reaction rate constants with X of OD-PABA and APAP, respectively, [X] is the steady-state concentration of the transient (note that OD-PABA and APAP are in the same solution), and [OD-PABA] = [APAP] = 10 µM are the initial concentration values of the two substrates. The equation can thus be simplified, and one gets that the ratio of the initial rates is equal to the ratio of the second-order rate constants. Therefore, by knowing the rate constant $k_{APAP,X}$ (De Laurentiis et al., 2014) and by measuring the initial degradation rates, one gets $k_{OD-PABA,X} = k_{APAP,X}\, R_{OD-PABA}(R_{APAP})^{-1}$.

The radical •OH was produced by irradiating 1 mM H_2O_2 under the TLK 05 or the TL 01 RS lamp, while anthraquinone-2-sulfonate (AQ2S) was used as CDOM proxy to study the reactivity of ^{3}CDOM* (De Laurentiis et al., 2014). In this case, 1 mM AQ2S was irradiated under the TLK 05

lamp. Measures of reactivity with $^1O_2$ were performed using a lamp Philips TL D 18W/16 with emission maximum at 545 nm. The dye Rose Bengal (10 µM initial concentration) was chosen as the $^1O_2$ source. Also in the indirect photolysis experiments, at the end of the irradiation, the content of the cells was recovered with 5 mL methanol. In all the cases, the pH of the irradiated solutions was 6-6.5.

2.2.3. Heterogeneous photocatalysis

A stock solution of OD-PABA was prepared in methanol at a concentration of 60 mg/L. The photocatalyst in powder form was then added to obtain a TiO_2 loading of 200 mg/L, after which the methanol solvent was evaporated in a Büchi Rotavapor system to allow the deposition of OD-PABA onto TiO_2. The recovery of the dry powder was carried out with ultrapure water. Five milliliters of the suspension thus obtained were introduced into cells of Pyrex glass and subjected to irradiation with a lamp Philips TLK 05 40 W, with emission maximum at 365 nm. After irradiation the content of the cells was recovered with 5 mL methanol (same reason as above) and filtered on a 0.45 µM syringe filter (hydrophilic PRFE, Millipore) to remove TiO_2. OD-PABA recovery was >90%.

2.3. Analytical techniques

2.3.1. High Performance Liquid Chromatography coupled with UV-vis detection

OD-PABA was monitored by using a VWR-Hitachi LaChrom Elite chromatograph, equipped with L-2300 autosampler (injection volume 60 µL), quatemary pump module L-2130, L-2300 column oven (temperature 40 °C), DAD detector L-2445, and a reverse-phase column (VWR RP-C18 LiChroCART, 4 mm × 125 mm × 5 µm). To determine both OD-PABA and APAP it was used a gradient of methanol and 3 mM phosphoric acid (1 mL/min flow rate), increasing the methanol

percentage from 15 to 90% in 15 min. The retention times were 3.1 and 12.4 min for APAP and OD-PABA, respectively; the column dead time was 1.1 min.

2.3.2. High Performance Liquid Chromatography coupled with High-Resolution Mass Spectrometry

HPLC-HRMS runs were carried out to identify the transformation intermediates. The chromatographic separations were run on a Phenomenex Luna 150 × 2.1 mm reverse-phase column (Phenomenex, Bologna, Italy), using an Ultimate 3000 HPLC instrument (Dionex, Milan, Italy). Injection volume was 20 μL and flow rate 200 μL/min. The elution used a gradient of the mixture A (acetonitrile) and B (0.05% v/v formic acid in water when run in ESI+ mode, 0.1 mM ammonium acetate in water for ESI–), passing from 5% to 100% A in 35 min.

A LTQ Orbitrap mass spectrometer (Thermo Scientific, Bremen, Germany) equipped with an atmospheric pressure interface and an ESI ion source was used. The LC column effluent was delivered into the ion source using nitrogen as both sheath and auxiliary gas. The tuning parameters adopted for the ESI source were: capillary voltage 37.00 V, tube lens 65 V. The source voltage was set to 3.5 kV. The heated capillary temperature was maintained at 275°C. The used acquisition method was optimised beforehand in the tuning sections for the parent compound (capillary, magnetic lenses and collimating octapole voltages) to achieve maximum sensitivity. Mass accuracy of the recorded ions (*vs.* calculated) was ± 10 millimass units (mmu) (without internal calibration).

Analyses were run using full MS (50-1000 *m/z* range), MS^2 and MS^3 acquisition in the positive ion mode, with a resolution of 30000 (500 m/z FWHM) in FTMS mode. The ions submitted to MS^n acquisition were chosen on the basis of full MS spectra abundance, without using automatic dependent scan. Collision energy was set to 30 (arbitrary units) for all of the MS^n acquisition methods. The MS^n acquisition range was between the values of ion trap cut-off and *m/z* of the fragmented ion. Xcalibur (Thermo Scientific, Bremen, Germany) software was used for both acquisition and elaboration.

2.4. Photochemical modeling

The assessment of the phototransformation kinetics was carried out with the APEX software (Aqueous Photochemistry of Environmentally-occurring Xenobiotics). It predicts photochemical half-life times as a function of water chemistry and depth, for compounds with known direct photolysis quantum yields and second-order reaction rate constants with transient species. APEX is based on a photochemical model, validated by comparison with field data of phototransformation kinetics in surface freshwaters (Bodrato and Vione, 2014).

APEX results apply to well-mixed water bodies, including the epilimnion of stratified lakes. The absorption of radiation by photosensitisers (CDOM, nitrate and nitrite) and xenobiotics is computed by taking into account competition for sunlight irradiance in a Lambert-Beer approach. Data obtained with APEX are averages over the water column of given depth, and they include the contributions of the well-illuminated surface layer and of darker water at the bottom. Therefore, results as a function of depth are not depth profiles but rather the comparison between different water bodies.

Sunlight irradiance is not constant in the natural environment, because of meteorological issues (not included in APEX) and of diurnal and seasonal cycles. To allow easier comparison between model results and environmental conditions, APEX uses as time unit a summer sunny day (SSD), equivalent to fair-weather 15 July at 45° N latitude. Another issue is that sunlight is not vertically incident over the water surface, but refraction at the interface deviates the light path in water towards the vertical. The light path length l depends on the depth d: on 15 July at 45°N it is $l = 1.05\ d$ at noon and $l = 1.17\ d$ at ±3 h from noon, which is a reasonable daily average (Bodrato and Vione, 2014).

3. Results and Discussion

3.1. Assessment of OD-PABA phototransformation in surface waters

When irradiated alone under the TL 01 RS lamp (emission maximum at 313 nm) under ~neutral pH conditions, 10 µM OD-PABA showed an initial degradation rate $R_{\text{OD-PABA}} = (3.48 \pm 0.24)\cdot10^{-10}$ M s^{-1}. The photon flux absorbed by OD-PABA was $P_a^{OD-PABA} = 4.5\cdot10^{-8}$ Einstein L^{-1} s^{-1}, which gives a direct photolysis quantum yield $\Phi_{OD-PABA} = (3.8 \pm 0.3)\cdot10^{-2}$. Because the used lamp shows an emission maximum that is very near the absorption maximum of OD-PABA (see Figure 1) and because the relevant band is also responsible for sunlight absorption, the calculated photolysis quantum yield would be representative of OD-PABA photodegradation under sunlight (Turro et al., 1978).

The reaction rate constant between OD-PABA and $^1O_2$ was measured by irradiating 10 µM OD-PABA and 10 µM APAP under the TL D 18W/16 lamp, in the presence of 10 µM Rose Bengal as $^1O_2$ source. Under the reported conditions it was $R_{\text{OD-PABA}} = (4.14 \pm 0.62)\cdot10^{-10}$ M s^{-1} and $R_{\text{APAP}} = (1.23 \pm 0.23)\cdot10^{-10}$ M s^{-1}. Considering that the second-order reaction rate constant $k_{APAP,^1O_2} = (3.68 \pm 0.73)\cdot10^7$ M^{-1} s^{-1} (De Laurentiis et al., 2014), one gets $k_{OD-PABA,^1O_2} = k_{APAP,^1O_2} R_{OD-PABA}(R_{APAP})^{-1} = (1.32 \pm 0.71)\cdot10^8$ M^{-1} s^{-1}.

Unfortunately it was not possible to measure the reaction rate constants of OD-PABA with •OH and ^{3}AQ2S* (taken as representative of ^{3}CDOM*), because irradiation under UVB and UVA caused an important direct photolysis of OD-PABA itself. Under such circumstances, equation (1) cannot be applied and the reaction rate constants cannot be determined. In the case of $^1O_2$, the measurement was allowed by the fact that the used lamp emits yellow light that is not absorbed by OD-PABA (which, therefore, underwent negligible direct photolysis under such conditions). In

spite of the experimental difficulties, reasonable values and upper limits for the reaction rate constants of OD-PABA with •OH and ^{3}CDOM* will be considered in photochemical modelling.

Figure 2 reports the modelled half-life time of OD-PABA (in SSD units, namely summer sunny days equivalent to 15 July at 45°N latitude) as a function of water depth *d* and of the dissolved organic carbon (DOC). The relevant calculations considered only the direct photolysis and the reaction with $^1O_2$, thus the results are actually upper limits for the lifetime of OD-PABA. Anyway, OD-PABA appears to be a rather photolabile compound, with lifetimes of less than one week even in reasonably deep (10 m) and high-DOC (~15 mgC L^{-1}) conditions. Interestingly, the phototransformation of OD-PABA would be almost exclusively accounted for by direct photolysis: the relative importance of the $^1O_2$ process would be always below 1%.

The figure shows that the half-life time increases with increasing depth and DOC. The former happens because the bottom layers of deep water bodies are poorly illuminated by sunlight and, therefore, they are poorly photoactive (Loiselle et al., 2008; Loiselle et al., 2009). On the other hand, high-DOC waters usually contain abundant CDOM that competes with the pollutants for sunlight irradiance, thereby inhibiting the direct photolysis processes (Vione et al., 2014).

As mentioned above, the reaction rate constants of OD-PABA with •OH and ^{3}CDOM* are unfortunately not available. They cannot have totally random values, however, because bimolecular reaction rate constants in aqueous solution have the diffusion control as an upper limit (Buxton et al., 1988). Therefore, an upper limit for the importance of OD-PABA phototransformation by •OH can be obtained by assuming $k_{OD-PABA,^{\bullet}OH} = 2 \cdot 10^{10}$ M^{-1} s^{-1} (diffusion-controlled reaction). Moreover, because ^{3}CDOM* is usually less reactive than •OH (Vione et al., 2014), $k_{OD-PABA,^3CDOM*}$ was assumed to vary between $1 \cdot 10^9$ and $1 \cdot 10^{10}$ M^{-1} s^{-1}. Figure 3 reports the fractions of the different photochemical pathways of OD-PABA as a function of the water DOC (assuming constant d = 5 m), with $k_{OD-PABA,^{\bullet}OH} = 2 \cdot 10^{10}$ M^{-1} s^{-1} and $k_{OD-PABA,^3CDOM*} = 1 \cdot 10^{10}$ M^{-1} s^{-1} (3a), as well as with

284 $k_{OD-PABA,^{\bullet}OH}$ = 2·10^{10} M^{-1} s^{-1} and $k_{OD-PABA,^{3}CDOM*}$ = 1·10^{9} M^{-1} s^{-1} (3b). In the former case the relative
285 role of $^{\bullet}$OH would always be lower than a few percent, and it would decrease with increasing DOC
286 (because of $^{\bullet}$OH scavenging by DOM), while the role of ^{3}CDOM* would increase with DOC
287 because ^{3}CDOM* is formed upon CDOM irradiation. Reaction with ^{3}CDOM* would account for
288 about one-quarter of OD-PABA phototransformation at DOC = 10 mgC L^{-1}. The direct photolysis
289 fraction would be maximum for DOC = 0.5-1 mgC L^{-1}, because of the role played by $^{\bullet}$OH at lower
290 DOC and by ^{3}CDOM* at higher DOC. In the case of Figure 3b, the direct photolysis is predicted to
291 always account for >95% of the OD-PABA phototransformation. In both cases, the minor role of
292 $^{\bullet}$OH implies that depth and DOC would be the main water parameters to control the
293 phototransformation of OD-PABA. Other parameters (nitrate, nitrite, inorganic carbon) would
294 mainly affect the $^{\bullet}$OH reactions and their expected role is minor.
295 Overall, one may conclude that the direct photolysis would be the main pathway leading to OD-
296 PABA photoattenuation in sunlit freshwaters, with a possibly significant role of ^{3}CDOM* under
297 high-DOC conditions. Therefore, first of all, the transformation intermediates arising from OD-
298 PABA direct photolysis were investigated.
299
300 **3.2. OD-PABA transformation intermediates arising upon direct photolysis**
301
302 Direct photolysis experiments were performed by subjecting an aqueous solution of OD-PABA to
303 UVA or UVB irradiation. Analysis was carried out in the ESI positive mode, which appeared to be
304 more sensitive and suitable for both the parent compound and most of the photogenerated
305 intermediates. Due to the low OD-PABA solubility in water, the aqueous solutions were prepared
306 by spiking with methanol or acetonitrile. As expected from substrate absorption and lamp emission,
307 UVB radiation was more effective than UVA to induce degradation: after 4 hours of irradiation,
308 90% of OD-PABA was degraded under UVB and only 20% under UVA.

Table S1 in the Supplementary Material (hereafter SM) shows the MS^2 and MS^3 OD-PABA product ions, useful to better identify the unknown transformation intermediates. A pattern of OD-PABA fragmentation, based on the information obtained in MS^2 and MS^3 spectra, is shown in Scheme 1. The MS^2 spectrum shows the formation of a product ion at 166.0862 *m/z* (formed by the loss of the alkyl chain) and of one at 151.0627 *m/z*, derived from the combined loss of the alkyl chain and a methyl radical.

The MS^3 study on the precursor ion 166.0862 *m/z* leads to the formation of the ion 151.0631 *m/z* as base peak, resulting from the loss of a methyl radical, and of the ion at 122.0964 *m/z* due to the loss of a molecule of carbon dioxide. The MS^3 study on the precursor ion 151.0627 *m/z* leads to the product ion 134.0600 *m/z*, formed through the loss of an OH radical. It has to be underlined that radical losses are not very common in a soft ionisation technique such as ESI (Geisow, 1990), although some cases have been recently documented (Medana et al., 2011; Sakkas et al., 2011).

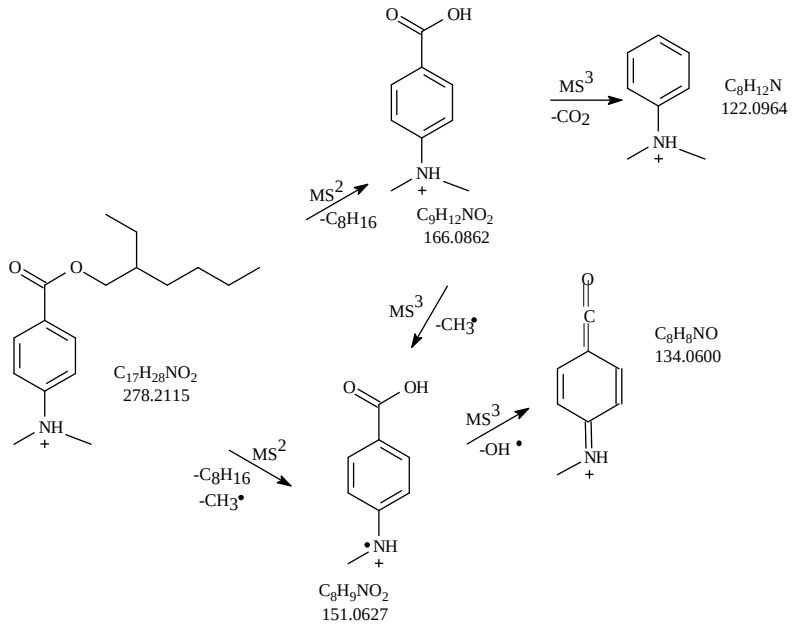

Scheme 1. Proposed fragmentation pathways of OD-PABA.

3.2.1. Identification of transformation intermediates

Five transformation intermediates were found under UVB irradiation (named from **I** to **V**) and four under UVA (**I** to **IV**). They are listed in Table 1, while their evolution profiles over time are shown in Figure 4. In all cases the most abundant compounds (as far as areas are concerned) were **I** (250.1799 *m/z*), **II** (292.1901) and **IV** (264.1954).

Compounds **I**, **III**, **IV**, **V** involved a dealkylation process. **I** and **IV,** with respective empirical formulas $C_{15}H_{24}NO_2$ and $C_{16}H_{26}NO_2$, showed in their MS^2 spectra the respective product ions 138.0546 and 152.0702 *m/z*, due to the loss of the unmodified alkyl chain. These structural-diagnostic ions suggest that dealkylation involved the amino group, with the detachment of one (or two) methyl groups (see Schemes S1 and S2 and Table S1 in the SM). Conversely, **III** (180.1014 *m/z*) and **V** (166.0863 *m/z*), with respective empirical formulas $C_{10}H_{14}NO_2$ and $C_9H_{12}NO_2$, were formed through the detachment of the alkyl chain. Considering compound **III**, the presence in its MS^2 spectrum of the structural-diagnostic ion with 148.0760 *m/z* and empirical formula $C_9H_{10}NO$ is crucial for the structure attribution. This product ion derives from the loss of methanol, thereby implying the presence of a methyl ester. Compound **V** shows a key product ion at 151.0628 *m/z*, due to the loss of a methyl radical. Its further fragmentation leads to the formation of 120.0444 *m/z*, resulting from the rearrangement of the molecule with elimination of a methoxy-radical. Therefore, compound **V** would result from OD-PABA by dealkylation of the alkyl chain and demethylation on the amino group. The proposed fragmentation pathway for 166.0863 *m/z* is shown in Scheme 2.

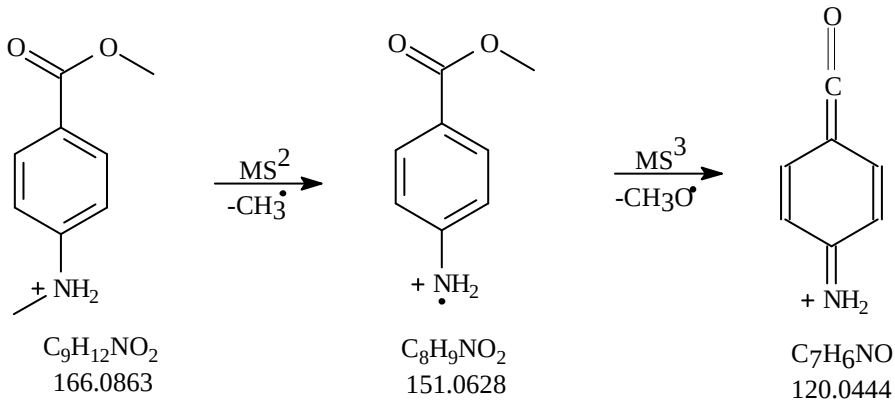

Scheme 2. Fragmentation pathway of 166.0863 *m/z* (compound **V**).

Compound **II,** with empirical formula $C_{17}H_{26}NO_3$, is well-matched with a monohydroxylated/oxidised derivative. The main product ion in the MS^2 spectrum is 180.0653 *m/z*, resulting from the loss of the unmodified alkyl chain. Therefore, the hydroxylation/oxidation takes place on the aromatic moiety of the molecule, reasonably involving one of the two methyl groups.

3.3. Transformation intermediates upon heterogeneous photocatalysis

Heterogeneous photocatalysis in the presence of TiO_2 in ultrapure water led to complete elimination of OD-PABA within 8 hours of irradiation. In these conditions (UVA irradiation) the direct photolysis would be a secondary pathway, *a fortiori* when taking into account the competition for lamp irradiance between OD-PABA and TiO_2. Along with substrate degradation, the formation of fourteen intermediate compounds occurred and their evolution profiles are plotted in Figure 5. In addition to the intermediates formed upon UVB irradiation, nine new compounds were identified (Table 1). In this case as well, the highest peak areas were observed for **I, II** and **IV**.

An additional dealkylated compound (**VII**), with 152.0706 *m/z* and empirical formula $C_8H_{10}NO_2$, was identified. The kinetic profiles suggest that it may be formed from **I** following a further demethylation. Compound **VI**, with 264.1594 *m/z* and empirical formula $C_{15}H_{22}NO_3$, was formed through the detachment of the two N-bonded methyl groups and an additional monohydroxylation/oxidation. The latter would probably occur on the alkyl chain, as suggested by the presence, in the MS^2 spectrum, of the product ion at 138.0550 *m/z* (see Table S1 in SM). The proposed fragmentation pathway is reported in Scheme 3.

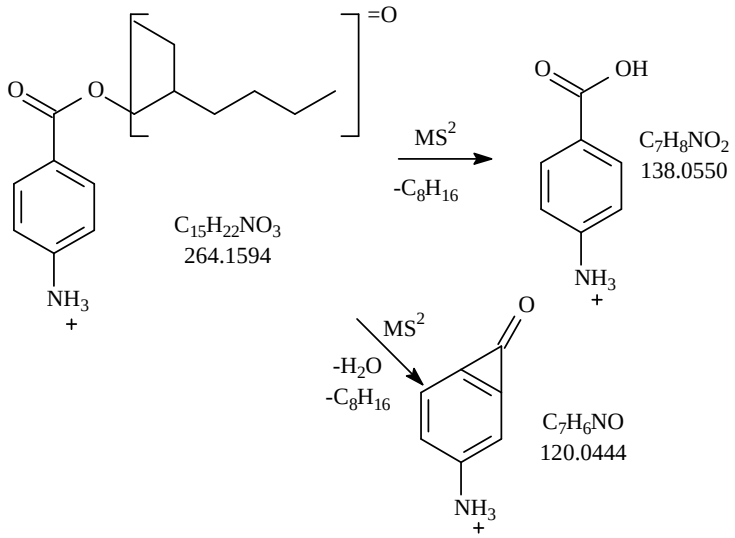

Scheme 3. Fragmentation pathway of 264.1594 *m/z* (**VI**).

Four species with 266.1741 *m/z* and empirical formula $C_{15}H_{24}NO_3$ (**VIII-XI)** can be attributed to dealkylated-hydroxylated derivatives. We attempted to characterise the four isobaric species *via* MS^n experiments. Compounds **VIII-X** share the same product ions, but with different relative intensities. They all have the structural diagnostic ion 138.0550 *m/z*, formed through the loss of $C_8H_{16}O$, which allowed to locate the hydroxylation on the alkyl chain. It was not possible, however, to discriminate the three isomers. Conversely, for compound **XI**, the presence in its MS^2 spectrum of the product ion 154.0502 *m/z* (Figure 6) allowed to locate the hydroxyl group on the aromatic moiety (see Table S2 in SM). The higher retention time of **XI** compared to **VIII-X** may be caused by the formation of a hydrogen bond between the hydrogen of the OH group and the carbonyl oxygen, which would be feasible only if the hydroxylation occurred on the *meta* position (with respect to NH_2) of the aromatic ring.

Three compounds with 306.1685 *m/z* and empirical formula $C_{17}H_{24}NO_4$ were identified and attributed to dihydroxylated/oxidised derivatives (**XII-XIV**). We attempted to characterise the three isomers through experiments of MS^2 and MS^3, and the product ions obtained are reported in Table S2 in SM. However, despite the abundance of information obtained from MS^n spectra, it was not possible to propose definite structures for these isomers.

3.4. OD-PABA transformation pathways

Figure 7 reports the proposed transformation pathways that link together all the characterised intermediates, resulting from OD-PABA photoinduced degradation under direct photolysis and heterogeneous photocatalysis.

The paths A (N demethylation), B (methyl group oxidation) and *a* (further demethylation) were the main transformation routes in all experimental conditions. Under UVA and UVB photolysis, the degradation of OD-PABA mainly occurred through reactions of demethylation. The identified intermediates would be formed following pathways A+*a* (**I**), B (**II**), C (**III**), A (**IV**), and C+*c* (**V**), where C is chain dealkylation and *c* is N demethylation. An analysis of the molecular structures leads to the suggestion that **I** would derive from **IV** and **V** from **III**. The photocatalysis experiments showed the formation of nine additional compounds (**VI**-**XIV**), not found upon direct photolysis. These additional TPs would arise from dealkylation (path *c'*), oxidation (path *b*) and demethylation-hydroxylation (paths *a'*, *a''*). Interestingly, the addition of TiO_2 would not induce the appearance of new primary transformation pathways for OD-PABA: it is hypothesised that the primary routes (A, B, C) would be the same as for the direct photolysis. The fact that different transformation pathways (photolysis *vs.* hydroxylation/oxidation) may yield similar intermediates has been frequently reported in this field of research (Vione et al., 2011; De Laurentiis et al., 2012; De Laurentiis et al., 2014). However, in the presence of TiO_2, there would be the additional transformation of **I** into **VI**, **VIII**, **IX**, **X** and **XI**, of **V** into **VII**, and of **II** into **XII**, **XIII** and **XIV**. The additional intermediates detected under photocatalytic conditions would thus be compounds formed by secondary or tertiary transformation. The fact that they were not detected in direct photolysis experiments could arise from the circumstance that, differently from OD-PABA, some of the early intermediates (and particularly **I**, **II** and **V**) might not undergo direct photolysis with elevated efficiency.

In the natural environment, where direct photolysis and possibly triplet-sensitised oxidation are expected to be the main OD-PABA transformation routes, the relevant pathways would be A, B, C to produce **II**, **III**, **IV**, followed by *a* and *c* to give **I** and **V**, respectively. Moreover, these primary and secondary intermediates might undergo a range of indirect photochemistry processes (reaction with •OH, $^1O_2$ and ^{3}CDOM*) to a variable extent. The hydroxylation and oxidation reactions are expected to be well foreseen by heterogeneous photocatalysis (Calza et al., 2010; Medana, et al., 2011b; Calza et al., 2013), probably yielding **VI-XIV** as additional intermediates in surface-water environments as well.

4. Conclusions

The sunscreen OD-PABA is expected to undergo direct photolysis as its main photochemical attenuation pathway in surface waters (with quantum yield $\Phi_{OD-PABA} = (3.8\pm0.3)\times10^{-2}$). Reactions with $^1O_2$ and •OH are certainly minor and/or negligible, while the present study is silent as to the precise importance of triplet-sensitised processes. However, an upper limit for ^{3}CDOM*-induced reactions can be placed at ~25% of total transformation, for d = 5 m and DOC = 10 mg C / L (the additional ~75% or higher of OD-PABA transformation would be accounted for almost exclusively by direct photolysis).

The main detected transformation intermediates of OD-PABA, at least as far as HPLC-HRMS peak areas are concerned, would be **I**, **II** and **IV** (where **I** is expected to arise upon **IV** transformation) in both direct photolysis and indirect phototransformation (the latter was simulated by using TiO_2-based heterogeneous photocatalysis). In the case of direct photolysis, an additional but less important pathway would yield **III** and, upon its transformation, **V**. A similar process would take place under photocatalytic conditions, which would also induce the following,

additional transformation processes: **I** → (**VI** + **VIII** + **IX** + **X** + **XI**); **V** → **VII**, and **II** → (**XII** + **XIII** + **XIV**). Photocatalysis was used here as a model system for indirect phototransformation, and intermediates **VI**-**XIV** could be formed for instance by triplet-sensitised oxidation. Further studies will be needed to confirm this assumption. The intermediates **VI**-**XIV** were not detected under direct photolysis, probably because **I**, **II** and **V** undergo direct photodegradation to a much lesser extent compared to OD-PABA. However, indirect photoprocesses are also operational in surface-water environments, where compounds **VI**-**XIV** might be formed as late transformation intermediates.

Acknowledgements

This work has been financed through the project funded by MIUR, in the frame of the collaborative international consortium WATERJPI2013-MOTREM of the Water Challenges for a Changing World Joint Programming Initiative (WaterJPI) Pilot Call. C.M. acknowledges financial support by the NANOMED project (PRIN 2010-2011, 2010FPTBSH_003) from Italian MIUR. D.V. also acknowledges financial support by Università di Torino / Compagnia di San Paolo - EU Accelerating Grants, project TO_Call2_2012_0047 (DOMNAMICS).

References

Bachelot, M., Li, Z., Munaron, D., Le Gall, P., Casellas, C., Fenet, H., Gomez, E., 2012. Organic UV filter concentrations in marine mussels from French coastal regions. Science of the Total Environment 420, 273-279

462 Balmer, M., Buser, H.R., Müller, M.D., Poiger, T., 2005. Occurrence of some organic UV filters in
463 wastewater, in surface waters, and in fish from Swiss lakes. Environmental Science and
464 Technology 39, 953–962
465 Bodrato, M., Vione, D., 2014. APEX (Aqueous Photochemistry of Environmentally occurring
466 Xenobiotics): A free software tool to predict the kinetics of photochemical processes in
467 surface waters. Environmental Science: Processes and Impacts 16, 732-740.
468 Braslavsky, S.E., 2007. Glossary of terms used in photochemistry. third edition. Pure and Applied
469 Chemistry 79, 293-465.
470 Calza, P., Medana, C., Raso, E., Gianotti, V., Minero, C., 2011. N,N-diethyl-m-toluamide
471 transformation in river water. Science of the Total Environment 409, 3894-3901
472 Calza, P., Marchisio, S., Medana, C., Baiocchi, C., 2010. Fate of the antibacterial spiramycin in
473 river waters. Analytical and Bioanalytical Chemistry 396 (4), 1539-1550
474 Calza, P., Medana, C., Padovano, E., Giancotti, V., Minero, C., 2013. Fate of selected
475 pharmaceuticals in river waters. Environmental Science and Pollution Research 20(4), 2262-
476 2270
477 Canonica, S., Kohn, T., Mac, M., Real, F. J., Wirz, J., Von Gunten, U., 2005. Photosensitizer
478 method to determine rate constants for the reaction of carbonate radical with organic
479 compounds. Environmental Science and Technology 39, 9182-9188.
480 Canonica, S., Hellrung, B., Müller, P., Wirz, J., 2006. Aqueous oxidation of phenylurea herbicides
481 by triplet aromatic ketones. Environmental Science and Technology 40, 6636-6641.
482 De Laurentiis, E., Chiron, S., Kouras-Hadef, S., Richard, C., Minella, M., Maurino, V., Minero, C.,
483 Vione, D., 2012. Photochemical fate of carbamazepine in surface freshwaters: Laboratory
484 measures and modeling. Environmental Science and Technology 46, 8164-8173.
485 De Laurentiis, E., Prasse, C., Ternes, T.A., Minella, M., Maurino, V., Minero, C., Sarakha, M.,
486 Brigante M., Vione D., 2014. Assessing the photochemical transformation pathways of

487 acetaminophen relevant to surface waters: Transformation kinetics, intermediates, and
488 modelling. Water Research 53, 235-248.
489 Diaz-Cruz, M.S., Gago-Ferrero, P., Llorca, M., Barcelo, D., 2012. Analysis of UV filters in tap
490 water and other clean waters in Spain. Analytical and Bioanalytical Chemistry 402(7), 2325-
491 2333
492 Fabbri, D., Minella, M., Maurino, V., Minero, C., Vione, D., 2015. Photochemical transformation
493 of phenylurea herbicides in surface waters: A model assessment of persistence, and
494 implications for the possible generation of hazardous intermediates. Chemosphere 119, 601-
495 607.
496 Fenner, K., Canonica, S., Wackett, L. P., Elsner, M., 2013. Evaluating pesticide degradation in the
497 environment: Blind spots and emerging opportunities. Science 341, 752-758.
498 Geisow, M., 1990. Electrospray ionization mass spectrometry - A powerful new analytical tool.
499 Trends in Biotechnology 8 (11), 303-311
500 Goksoyr, A., Tollefsen, K.E., Grung, M., Loken, K., Lie, E., Zenker, A., 2009. Balsa raft crossing
501 the Pacific finds low contaminant levels. Environmental Science and Technology 43, 4783–90
502 Gomez, E., Pillon, A., Fenet, H., Rosain, D., Duchesne, M. J., Nicolas, J. C., Balaguer, P., Casellas,
503 C., 2005. Estrogenic activity of cosmetic components in reporter cell lines: Parabens, UV
504 screens, and musks. Journal of Toxicology and Environmental Health A 68 (4), 239-251
505 Kameda, Y., Kimura, K., Miyazaki, M., 2011. Occurrence and profiles of organic sunblocking
506 agents in surface waters and sediments in Japanese rivers and lakes. Environmental Pollution
507 159, 1570–1576
508 Kupper, T., Plagellat, C., Brändli, R.C., de Alencastro, L.F., Grandjean, D., Tarradellas, J., 2006.
509 Fate and removal of polycyclic musks, UV filters and biocides during wastewater treatment.
510 Water Research 40, 2603–2612
511 Leon-Gonzalez, Z., Ferreiro-Vera, C., Priego-Capote, F., Luque de Castro, M.D., 2011. Targeting
512 metabolomics analysis of the sunscreen agent 2-ethylhexyl 4-(N,N-dimethylamino)benzoate

513 in human urine by automated on-line solid-phase extraction-liquid chromatography-tandem
514 mass spectrometry with liquid chromatography-time-of-flight/mass spectrometry
515 confirmation. Journal of Chromatography A 1218, 3013-3021
516 Li, W., Ma, Y., Guo, C., Hu, W., Liu, K., Wang, Y., Zhu, T., 2007. Occurrence and behavior of
517 four of the most used sunscreen UV filters in a wastewater reclamation plant. Water Research
518 41, 3506 – 3512
519 Loiselle, S. A., Azza, N., Cozar, A., Bracchini, L., Tognazzi, A., Dattilo, A., Rossi, C., 2008.
520 Variability in factors causing light attenuation in Lake Victoria. Freshwater Biology 53, 535-
521 545.
522 Loiselle, S. A., Bracchini, L., Dattilo, A. M., Ricci, M., Tognazzi, A., Cozar, A., Rossi, C., 2009.
523 Optical characterization of chromophoric dissolved organic matter using wavelength
524 distribution of absorption spectral slopes. Limnology and Oceanography 54, 590-597.
525 Magi, E., Scapolla, C., Di Carro, M., Rivaro, P., Kieu, T. N. N., 2013. Emerging pollutants in
526 aquatic environments: monitoring of UV filters in urban wastewater treatment plants.
527 Analytical Methods 5(2), 428-433
528 Marchetti, G., Minella, M., Maurino, V., Minero, C., Vione, D., 2013. Photochemical
529 transformation of atrazine and formation of photointermediates under conditions relevant to
530 sunlit surface waters: Laboratory measures and modelling. Water Research 47, 6211-6222.
531 Medana, C., Calza, P., Deagostino, A., Dal Bello, F., Raso, E., Baiocchi, C., 2011a. ESI $HRMS^n$
532 fragmentation pathways of phenazone, an N-heterocyclic drug compound. Journal of Mass
533 Spectrometry 46, 782–786
534 Medana, C., Calza, P., Dal Bello, F., Raso, E., Minero, C., Baiocchi, C., 2011b. Multiple unknown
535 degradants generated from the insect repellent DEET by photoinduced processes on TiO_2.
536 Journal of Mass Spectrometry 46, 24–40
537 Mostafa, S., Rosario-Ortiz, F. L., 2013. Singlet oxygen formation from wastewater organic matter.
538 Environmental Science and Technology 47, 8179-8186.

539 Mostafa, S., Korak, J. A., Shimabuku, K., Glover, C. M., Rosario-Ortiz, F. L., 2014. Relation
540 between optical properties and formation of reactive intermediates from different size
541 fractions of organic matter. In: Advances in the Physicochemical Characterization of
542 dissolved Organic Matter: Impact on Natural and Engineered Systems. Rosario-Ortiz, F. L.
543 (ed.), ACS Symposium Series, Vol. 1160, pp. 159-179.
544 Poiger, T., Buser, H.R., Balmer, M.E., Bergqvist, P.A., Müller, M.D., 2004. Occurrence of UV
545 filter compounds from sunscreens in surface waters: regional mass balance in two Swiss lakes.
546 Chemosphere 55, 951–963
547 Rodil, R., Moeder, M., 2008. Development of a method for the determination of UV filters in water
548 samples using stir bar sorptive extraction and thermal desorption–gas chromatography–mass
549 spectrometry. Journal of Chromatography A 1179, 81–88
550 Rodil, R., Moeder, M., Altenburger, R., Schmitt-Jansen, M., 2009. Photostability and phytotoxicity
551 of selected sunscreen agents and their degradation mixtures in water. Analytical and
552 Bioanalytical Chemistry 395, 1513–1524
553 Sakkas, V. A., Calza, P., Vlachou, A. D., Medana, C., Minero, C., Albanis T., 2011. Photocatalytic
554 transformation of flufenacet over TiO_2 aqueous suspensions: Identification of intermediates
555 and the mechanism involved. Applied Catalysis B: Environmental 110, 238– 250
556 Schlumpf, M., Cotton, B., Conscience, M., Haller, V., Steinmann, B., Lichtensteiger, W., 2001. In
557 vitro and in vivo estrogenicity of UV screens. Environmental Health Perspecitves 109 (3),
558 239-244.
559 Tunkel, J., Mayo, K., Austin, C., Hickerson, A., Howard, P., 2005. Practical considerations on the
560 use of predictive models for regulatory purposes. Environmental Science and Technology 39,
561 2188-2199.
562 Vione, D., Maddigapu, P. R., De Laurentiis, E., Minella, M., Pazzi, M., Maurino, V., Minero, C.,
563 Kouras, S., Richard, C., 2011. Modelling the photochemical fate of ibuprofen in surface
564 waters. Water Research 45, 6725-6736.

565 Vione, D., Minella, M., Maurino, V., Minero, C., 2014. Indirect photochemistry in sunlit surface
566 waters: Photoinduced production of reactive transient species. Chemistry: A European Journal
567 20, 10590-10606.
568 Wenk, J., Eustis, S. N., McNeill, K., Canonica, S., 2013. Quenching of excited triplet states by
569 dissolved natural organic matter. Environmental Science and Technology 47, 12802-12810.
570

571 **Table 1.** List of $[M+H]^+$ obtained from OD-PABA and its intermediate compounds (the time trends
572 of the latter are reported in Fig. 4 and 5).

573

574

$[M+H]^+$ and empirical formula	**Name**	**Isomer**	**Δmmu**	**t_R (min)**
278.2115 $C_{17}H_{28}NO_2$	**OD-PABA**		0.665	36.0
250.1799 $C_{15}H_{24}NO_2$	**I**	-	0.294	30.7
292.1901 $C_{17}H_{26}NO_3$	**II**	-	-0.380	31.4
180.1014 $C_{10}H_{14}NO_2$	**III**	-	-0.495	22.3
264.1954 $C_{16}H_{26}NO_2$	**IV**	-	-0.376	33.4
166.0863 $C_9H_{12}NO_2$	**V**	-	-0.635	18.7
264.1594 $C_{15}H_{22}NO_3$	**VI**	-	-1.190	23.5
152.0706 $C_8H_{10}NO_2$	**VII**	-	-0.535	14.3
266.1741 $C_{15}H_{24}NO_3$	**VIII**	**266 A**	-0.940	19.9
266.1741 $C_{15}H_{24}NO_3$	**IX**	**266 B**	-0.940	21.7
266.1741 $C_{15}H_{24}NO_3$	**X**	**266 C**	-0.940	22.4
266.1741 $C_{15}H_{24}NO_3$	**XI**	**266 D**	-0.940	27.5
306.1685 $C_{17}H_{24}NO_4$	**XII**	**306 A**	-1.525	21.7
306.1685 $C_{17}H_{24}NO_4$	**XIII**	**306 B**	-1.525	22.8
306.1685 $C_{17}H_{24}NO_4$	**XIV**	**306 C**	-1.525	23.8

575

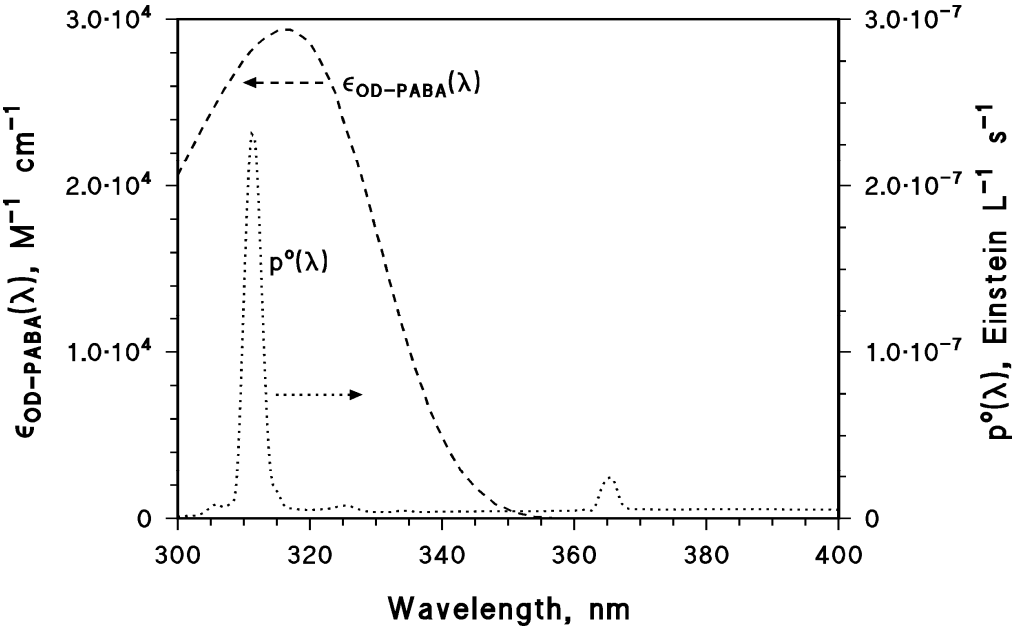

Figure 1. Absorption spectrum (molar absorption coefficient $\varepsilon_{OD-PABA}(\lambda)$) of OD-PABA. Emission spectrum (spectral photon flux density p°(λ)) of the TL 01 RS lamp.

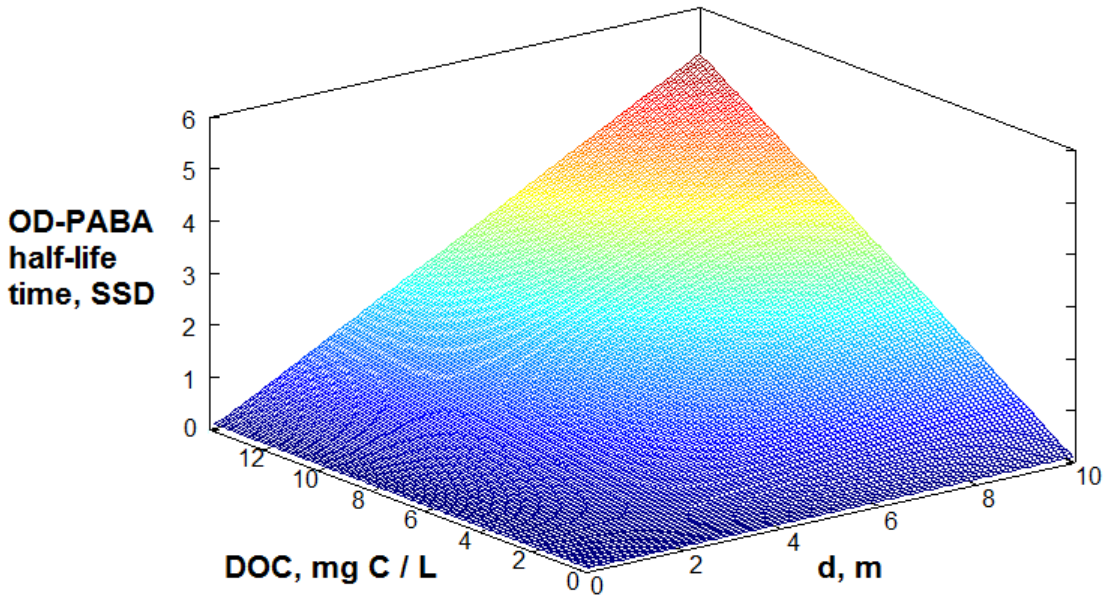

Figure 2. Modelled half-life time of OD-PABA (units of SSD = summer sunny days equivalent to 15 July at 45°N latitude) as a function of water depth and DOC. Other water conditions: 0.1 mM nitrate, 1 µM nitrite, 1 mM bicarbonate, 10 µM carbonate.

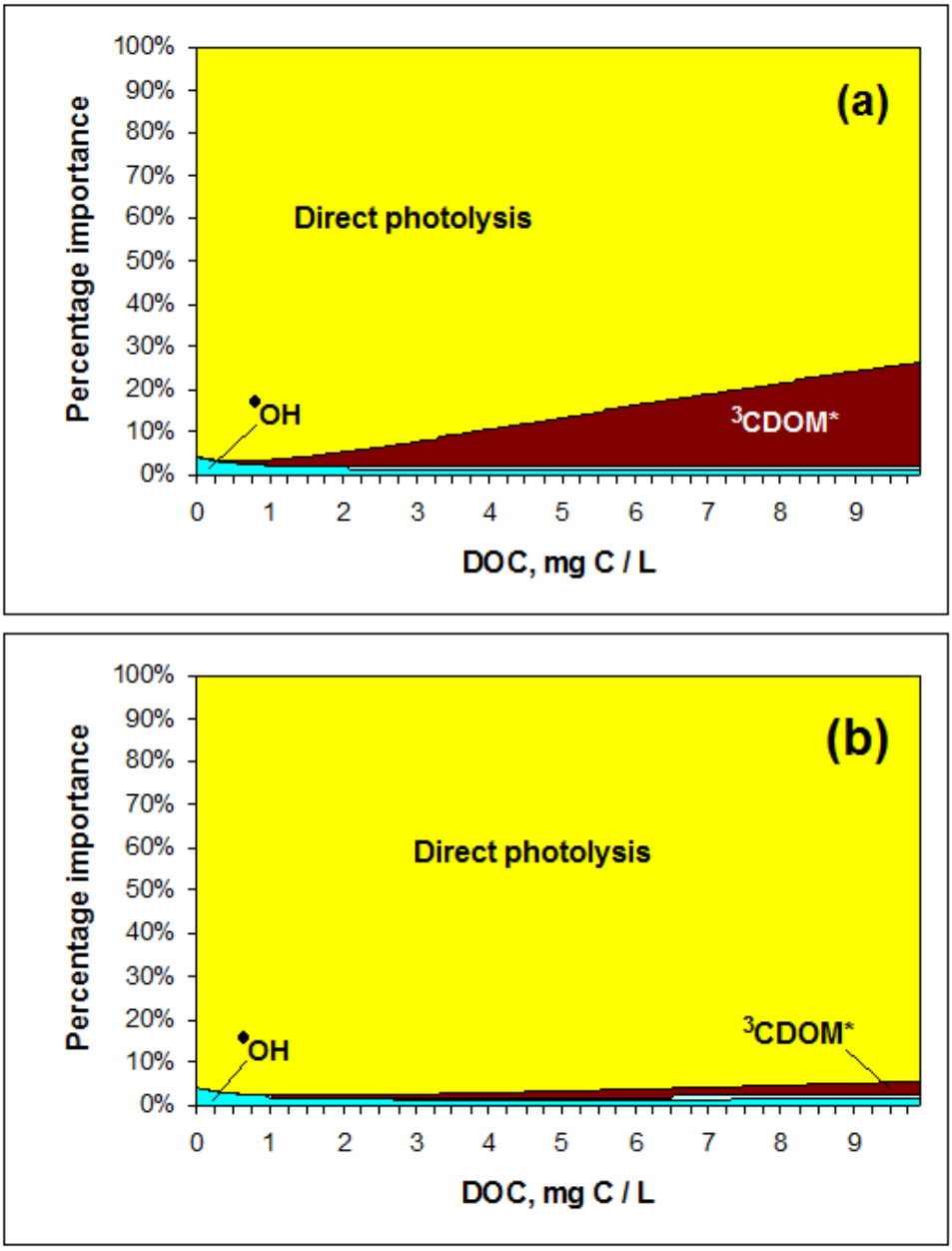

Figure 3. Relative (modelled) role of the different photochemical processes in the transformation of OD-PABA, as a function of the water DOC. It was assumed $k_{OD-PABA,^{\bullet}OH}$ = $2 \cdot 10^{10}$ M^{-1} s^{-1} (both cases) and $k_{OD-PABA,^{3}CDOM^{*}}$ = $1 \cdot 10^{10}$ M^{-1} s^{-1} (3a) or $1 \cdot 10^{9}$ M^{-1} s^{-1} (3b). Other water conditions: 5 m depth, 0.1 mM nitrate, 1 µM nitrite, 1 mM bicarbonate, 10 µM carbonate.

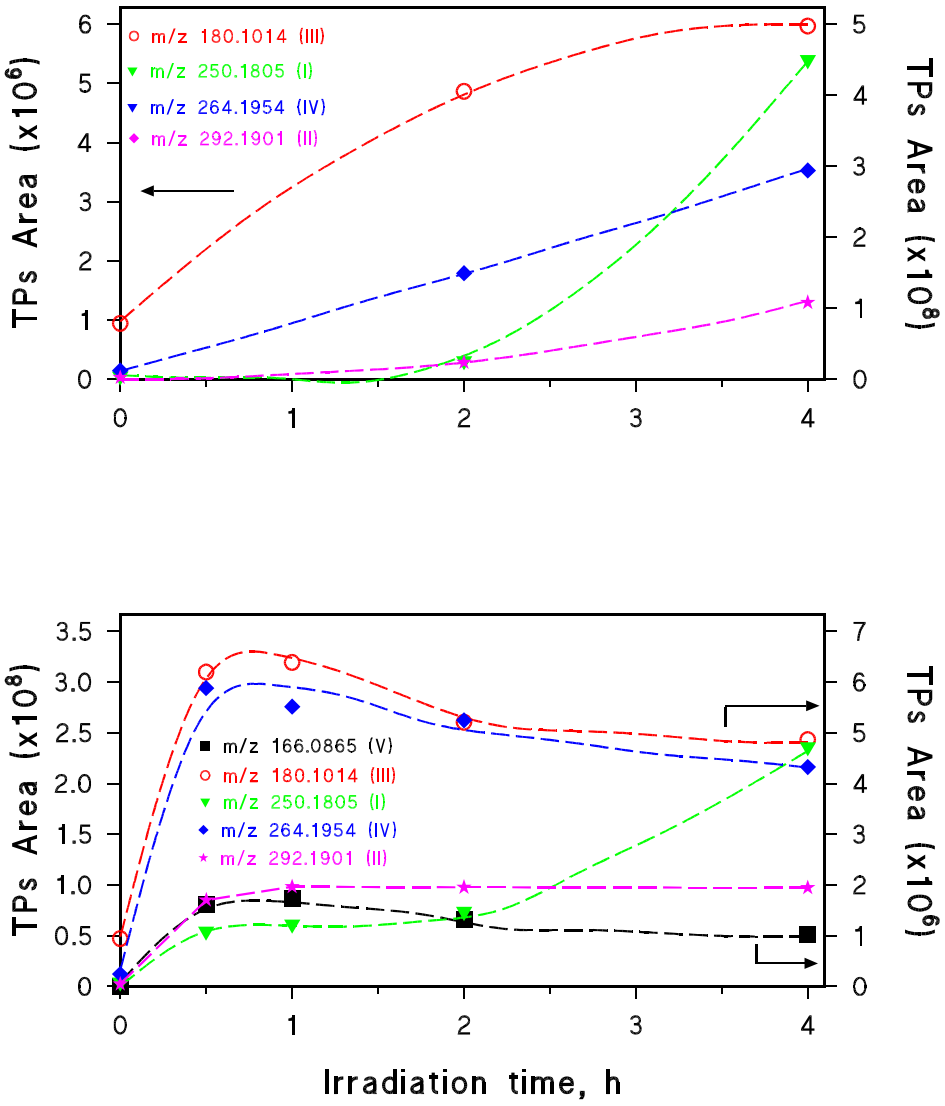

Figure 4. Evolution of the OD-PABA TPs formed over time upon direct photolysis, under UV-A (top) and UV-B (bottom) irradiation. Note the different Y-axis scales for different intermediates: the arrows indicate the Y-axis against which the relevant time profiles are plotted (those without the arrow are plotted against the opposite axis).

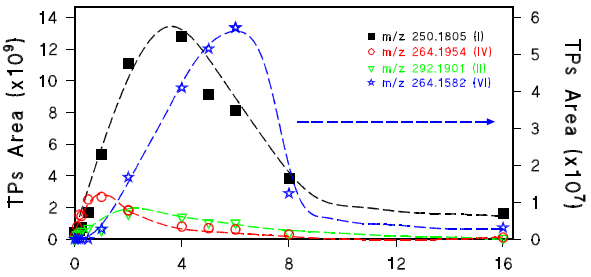

607

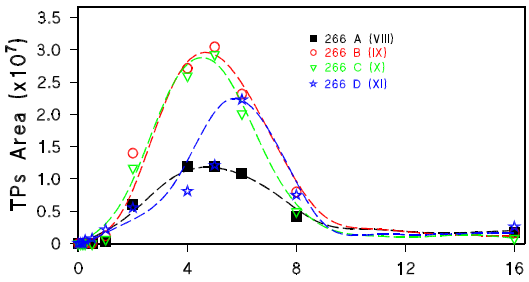

608

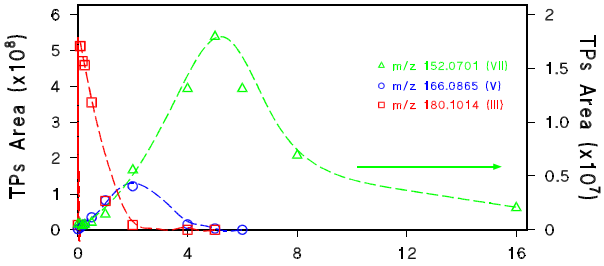

609

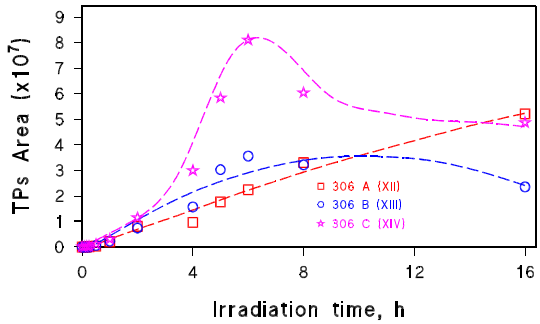

610

611

612 **Figure 5.** Evolution of PABA TPs over time, formed under heterogeneous photocatalysis. The
613 meaning of the arrows is the same as for Figure 4.

614

615

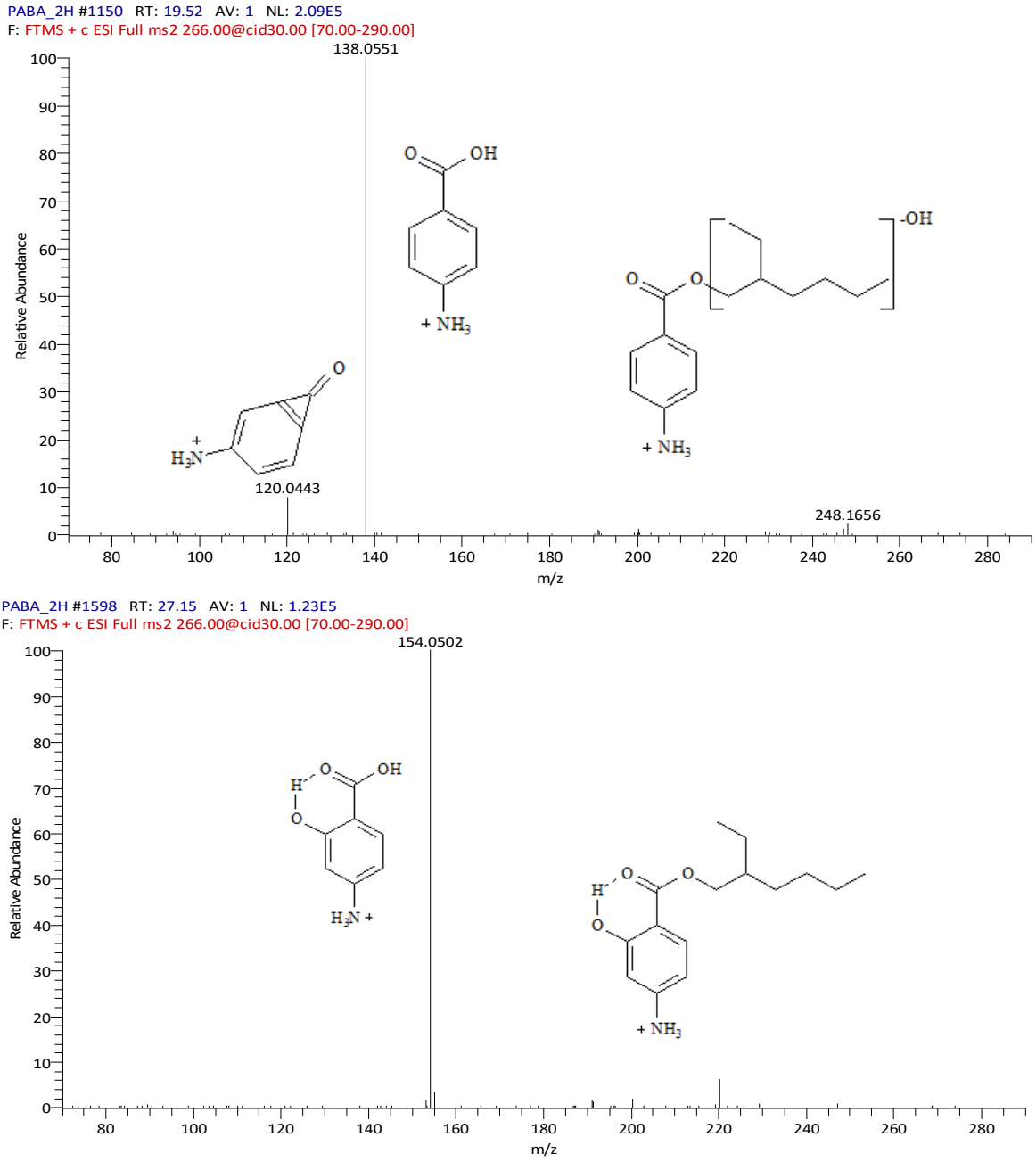

616

617

618 **Figure 6.** MS^2 spectrum for: *top*) isomer **VIII**, *bottom*) isomer **XI**.

619

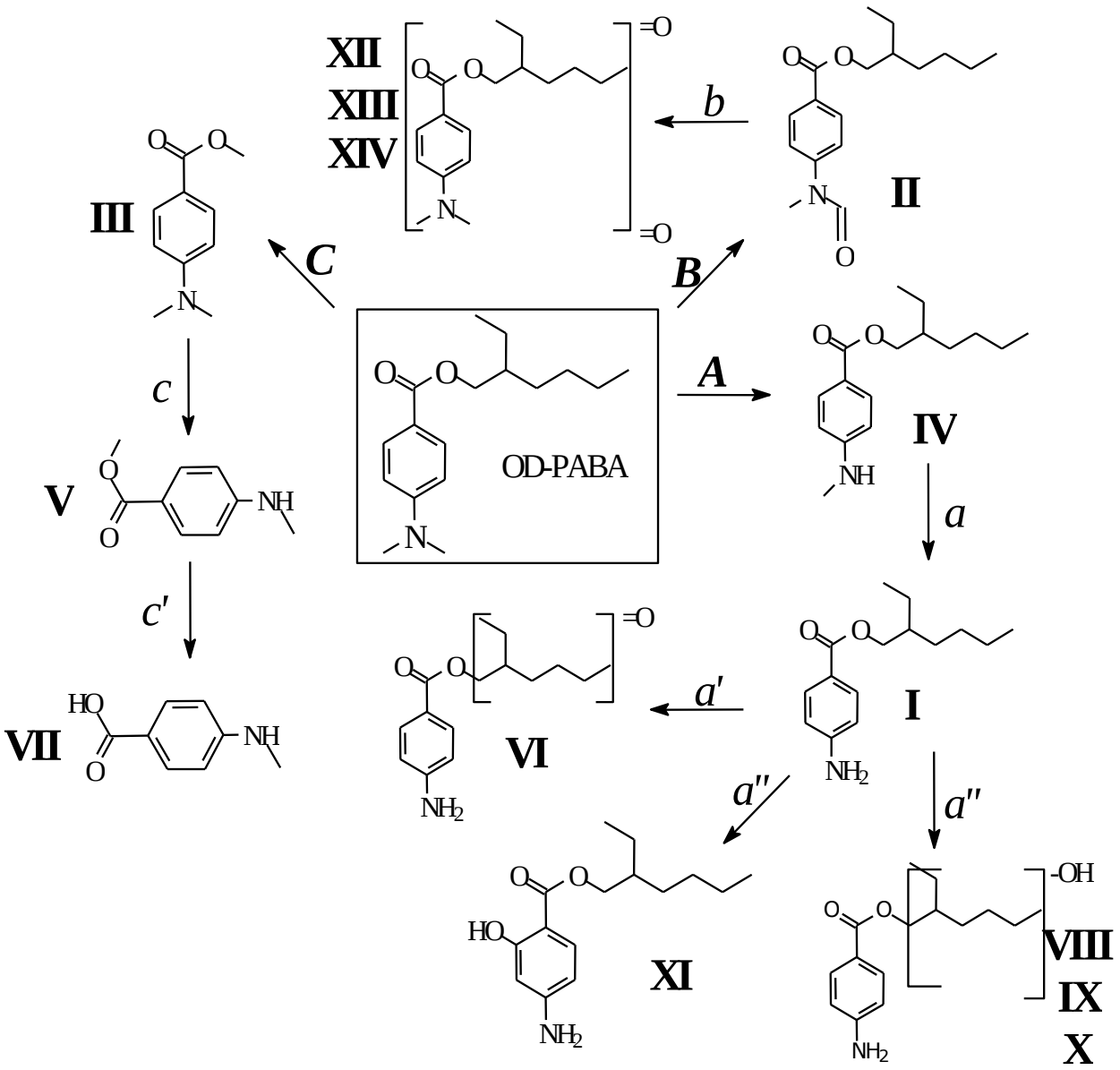

Figure 7. Proposed transformation pathways followed by OD-PABA under direct photolysis and heterogeneous photocatalysis